PSIG 1910

A mathematical model for the spatial prediction and temporal evolution of the column separation in a flowing hydrocarbon transmission pipeline

Hamed Ghasvari Jahromi, Fatemeh Ekram, Michael Roxas, Satya Mokamati

Vanmok Leak Detection Technologies Inc.

This paper was prepared for presentation at the PSIG Annual Meeting held in London, England, 14 May – 17 May 2019.

ABSTRACT

A novel model is used to predict the inception moment and location of a phenomenon known as the column separation or slack line. The existing models for prediction of the cavitation phenomenon in internal flow systems in general are primarily formulated for the capture of the inception moment and initial location of the event only. Hence questions such as where the incepted cavities and bubbles tend to go, or the detailed state of a slack line in time should be addressed using a different approach.

The model presented in this paper is validated and verified against experimental data available in the literature before being applied to a 53 Km (33 miles) industrial pipeline. Imposing conditions at the injection and delivery ends of the line tests various scenarios causing column separation. Hydraulic parameters such as pressure head and flowrate as well as interfacial mass transfer rate of the incepting and collapsing bubbles and cavity zones are predicted in real time over the entire domain of space and time.

The results predicted the fate of the separated column of the fluid, whether they rejoin or continue to change the size with different rates or even if they become stabilized stationary cavity pockets after passage of minutes or hours. Results are also compared based on the initial cause of the column separation such as huge transients. Also, accurate prediction of the whole column separation event, distinguishes it from other events, which would commonly mimic or mask the column separation by exhibiting identical hydraulic footprints.

INTRODUCTION AND BACKGROUND

It should be kept in mind that column separation is used in this paper in a broader definition range, all the way from local cavitation to intermediate cavities as well as propagation of the near wall formed vaporous cavitation zones. Therefore "column separation" or "slack line" in this paper refers to both above-mentioned possible outcomes. The liquid hold-up (or liquid fraction) can change as a function of space and time, and thermodynamically only constrained to one condition which is saturated vapor pressure at the given temperature for the phase change moment and location [1].

A transient-state in the system (such as sudden pump failure or valve closure, or drastic set point changes to control the flow in the pipeline) or rapid elevation gain of the pipeline are some of the reasons that could provide the favorable condition for cavity formation. Another important category under which the cavitation may occur is when the pipeline which contains the fluid, undergoes a substantial enough amount of heat transfer with its surrounding such that the pressure inside the pipeline falls below the value of vapor pressure (dictated by the thermodynamic equilibrium state that system and the surrounding wish to reach) [1]. These are all causes of column separation for a closed control volume of the pipeline system. If the control volume being allowed to have mass fluxes at other locations except it's both ends, it means that cases of injection or leak can occur. This is the most challenging and yet most crucial one to be addressed as the similarities between the signature of a leak event and column separation can cause masking of the leak or in accuracies in the computations of slack if the leak remains undetected. The mechanism that causes column separation during leak events is not fundamentally different than the rest. Cause of pressure drop to the vicinity of vapor pressure at the given temperature is loss of energy at the leak spot to the ambient.

Due to any of the above-mentioned reasons, when favorable condition for cavity formation begins, the small vapor-filled cavities can grow to bigger cavities and potentially (depending on pipeline configuration or transient-state in the system), lead

to one or both the following [1]:

1. Create a thin cavity confined to the top of the pipe extending over a long distance; referred to a condition known as cavitating flow.
2. To fill the entire cross section of the pipe and thus divide the liquid into two columns; referred to a condition known as column separation.

APPROACH

REVIEW OF THE CURRENT APPROACHES; NEED FOR A NOVEL MODEL

Most common approaches to the column separation problem is reviewed in the literature by Bergant et al [2] and the issue with these approaches are explained by Ghasvari Jahromi et al [1] with a comparison conducted between the results from the conventional methods and the results from the novel approach undertaken in this study.

The target in choice of the right model is to be assured of the rigorousness of the underlying mathematics of the model in terms of its synchrony with the experimental data.

It is possible for experimental scientists when dealing with much smaller characteristic lengths (dozens of meters to couple of hundred meters in length) to report the inception time and location, duration of existence and growth or final death of the incepted cavities.

The level of agreement between the results of any model at small-scale experiments is the key factor in choosing the right model for industrial scale pipelines.

The verification and validation of a mathematical model against appropriate experimental data is very important to believe in the model that can address the pipeline operations related issues with confidence. The critical evaluations should address the operational questions such as, where the incepted cavities and bubbles tend to go in larger pipeline systems? or what is the detailed state of the slack line? After the verification and validation, the rigorousness of the model and the robustness of the numerical methods used to solve it could be claimed as accurate. Fortunately, experimental data for such purposes can be found in the literature for the validation purposes.

Our criteria for selecting the appropriate experimental data is studies with direct measurements and no bias towards any of the conventional models (in cases where the experiments were compared to mathematical models).

The work of Bergant et al [3] is chosen due to the comparisons made between their own measured experimental data and the most common models used for the column separation. This work does not report anything about the vaporous phase directly. However, it provides the measurements of pressure head, flowrates and the predictions of them by each of the three conventional models considered in their study. This provides an important benchmark for column separation models to be compared against. Comparisons with this work can shed some light onto whether each model's prediction of events (for example time and location of the highest-pressure peak in the system) remains synched with the experiments.

The work of Sanada et al [4] is chosen due to direct measurements of the "inception time and location" and "duration of existence and final fate of the incepted cavities". This provides an important benchmark for any model who wants to predict the slack line in real time accurately. Using this work, it will be possible for any model to be compared against experimental results for the predicted temporal and spatial evolution of the phase change.

NOVEL MATHEMATICAL MODEL

The constitutive equations between pressure and temperature and in some cases, even fluid properties such as vapor density and viscosity for various hydrocarbon products are not clearly known. Therefore, we had provided the governing equations with functional forms for the case of transient-thermal model [1]. Since the effect of these parameters are unknown, they are grouped into functional forms. These functional forms allow for the tuning of the model in the practical implementations.

$$\frac{1}{c^2}\frac{\partial P}{\partial t} + f_1(\varphi, x, t)\frac{\partial Q^*}{\partial x} + f_2(x, t, \Delta\rho) = 0 \quad (1)$$

$$\frac{\partial Q^*}{\partial t} + \left(\frac{1}{f_1(\varphi, x, t)}\right)\frac{\partial P}{\partial x} + f_3(z, \varphi, t)) + f_4(Q^*, \varphi) = 0 \quad (2)$$

$$(3):$$

$$\frac{\partial T}{\partial t} + \frac{1}{A_0}\frac{\partial (QT)}{\partial t} = \frac{k}{\rho c_p}\left[\frac{\partial^2 T}{\partial x^2} + \frac{dA_c}{A_c dx}\frac{\partial T}{\partial x}\right] + \frac{U_\infty}{\rho c_p}\left(\frac{P_i}{A_c}\right)(T_\infty - T)$$

$$a_1 = f_5(k_l, r, \delta, E, \rho) \quad (4)$$

System of coupled equations (1,2,3 and 4) are such generic functional representation of the conservation of mass and momentum, used by Ghasvari Jahromi et al [1] for the case where the pipeline is subjected to long hours of cooling during shut-in. Correctional functionals are f_1, f_2, f_3, and f_4 and they are not known a priori. This allows the model to be able to capture the operational activities that a realistic computational pipeline model need.

Functional name	independent variables and functions
f_1	Space, time and density
f_2	Space, time and density margin to vapor
f_3	Space, elevation
f_4	Flowrate, friction factor and density
f_5	Bulk modulus of the fluid, Young's modulus of the pipe, wall thickness of the pipe, pipe inner diameter and density of the fluid

Aside from transient thermal cases, other operational activities such as multi-batch flow, variable fluid properties of each batch and use of drag reductant agent (DRA) are a few other examples, which clearly require a model with the functional form degree of freedom.

Description of functionals in the equations
f_1: compressibility functional coefficient
f_2: interphase mass transfer functional term
f_3: Momentum losses correcting functional term
f_4: Momentum residual correcting functional term
f_5: Constitutive functional form

This approach can be used to address complicated scenarios where the effects of temperature or unknown properties are important in the accuracy of the results. We refer the reader to Ghasvari Jahromi et al [1] for further explanations and the results of this approach on a non-flowing line subjected to long hours of cooling during shut-in.

We assumed isothermal condition for the cases studied in this paper. Therefore, we skip the first law of thermodynamics for the model used in this paper and we use the general conservation laws for mass and momentum only instead of using the functional form of these governing equations with the energy equation.

$$\frac{D\rho}{Dt} + \rho\nabla \cdot u = \sigma \tag{5}$$

$$\frac{\partial\rho}{\partial t} + \nabla \cdot (\rho u) = \sigma \tag{6}$$

$$c = \sqrt{\left(\frac{\partial P}{\partial \rho}\right)_s} \tag{7}$$

$$c = \sqrt{\frac{k_l}{\rho_l + \frac{Dk_l\rho_l}{Ee}}} \tag{8}$$

$$\frac{D(\rho u)}{Dt} = -\nabla P + \nabla \cdot \tau + \rho f_x + \beta \tag{9}$$

Equation (5) is the physical law of conservation of mass in its most general form. The first term is the substantial derivative of the fluid density which consists of the two terms itself: temporal density changes with time and advective density changes with space. The divergence term can be combined with the advective term to form the flux conservative form of the continuity equation as is shown in equation (6).

Equation (7) is general constitutive equation which states the pressure wave speed in the fluid. Pressure wave speed in the fluid is the square root of density rate of change of the pressure isentropically. This in fact is the equation of the state of the model, which due to hyperbolic nature of this coupled system of partial differential equations, plays an important role in the solution strategy.

In other words, it can become analogous to an extra constraint on the system where condition on CFL[1] number must be applied. Physically speaking the simultaneity between the model and the real world will be kept only if numerical discretization of the temporal and spatial variables considers the characteristic nature of speed of sound for this transient model. Equation (8), then will correlate this consideration to some of the material properties of both the fluid and the pipeline in which the fluid flows.

Equation (9) is the physical law of conservation of momentum in its most general form. The term on left hand side is the total derivative of the momentum within the control volume. The right-hand side has the pressure gradient term, divergence term of the shear stress (which is for surface forces due to shear stress at the walls). The last two terms consider the body forces due to gravity for non-horizontal profiles and residual momentums respectively (that could be non-zero if

[1] Courant–Friedrichs–Lewy (CFL) is a necessary condition for convergence while solving mostly hyperbolic PDEs numerically.

injection or losses are known to be likely to happen).
A new form of the continuity equation appears by using Equation (10), (which is simply the chain rule between density and pressure) with the speed of sound and temporal pressure term instead of density.

$$\frac{\partial P}{\partial t} = \frac{\partial \rho}{\partial t} \cdot \frac{\partial P}{\partial \rho} \tag{10}$$

Equation (11) shows the transient momentum equation for a one-dimensional, unidirectional flow in the pipeline with variable density and friction factor used in the representation of the viscous losses.

$$\frac{1}{c^2}\frac{\partial P}{\partial t} + \frac{\partial(\rho u)}{\partial x} = \sigma \tag{11}$$

$$\frac{D(\rho u)}{Dt} + \frac{\partial P}{\partial x} + \frac{(\rho_l - \rho_v)^2 \rho_l f^*}{2D(\rho - \rho_v)} u|u| + \rho f_x - \beta = 0 \tag{12}$$

Right hand side of Equations (5,6,11) as well as the last term in the Equation (12), become zero if no injection or losses (i.e. sinks and sources) exist within the system. The phase change originating from a leak incident has been remained as one of challenging problems in the applied hydraulic engineering. However, since phase change due to leak is one of the interesting scenarios of column separation which we considered in this paper, these mentioned terms are kept in these equations and are not set to zero.

COLUMN SEPARATION CONDITIONS

Following is the list of main hydraulic causes of slack line or column separation.

1. Column separation due to sudden[2] valve closure.
2. Mid-stream cavitation due to pressure transients.
3. Column separation due to cooling during extended shut-in periods.
4. Column separation due to shut-down.
5. Column separation due to setpoint change on a pipeline with huge gradients in its elevation profile.
6. Column separation due to out of segment rupture incident.
7. Column separation due to leak.

First one has been addressed using the current model in [1] as a validation test study against experimental results of Bergant et al. [3] on a 37-meter inclined pipeline with positive and negative slopes. They showed the pressure head and flow rates during the event of the valve closure at upstream and downstream ends separately using conventional models[3]. While these models have all shown success in the capture of inception moment and location of the phase change due to valve closure, only the complicated to implement model of gas vapor interface cavity could predict the maximum pules in the pressure without overshoots in the value of it. All models failed to provide a direct variable which is calculated during the solution at all nodes and time steps for the density and phase change. That is the main reason that predictions of vapor are not provided in their study. Also, all these conventional models even GIVCM has shown to go out of synchrony with experimental result only a few seconds into the simulation. The results of the novel model were compared [1] with the same experimental results provided by Bergant et al. [2] to show that the solution of the vapor phase as an independent density based calculated parameter, and with the modification of variable friction factor, fixes not only the overshoot problem in predicting the peak of pressure pulses due to column separation, but it also remains synchronized with the experimental results and the location of the maximums and minimums and the trend of the elevation head matches with the experimental results (without lag) with very high accuracy.

Second cause in the list is also used for validation purposes, in [1]. The experimental results of Sanada et al [4] were used which had two advantages compared to the previous case to be chosen for validation purpose. Not only it was a different yet simpler cause behind the column separation, but they were able to provide not only velocity and pressure measurements of their experiment but also their measurements of the birth and death time of the incepted bubbles in the mid-section of a 200-m-long horizontal PVC pipe, as well. This is a guaranteed benchmark case for validation as the valve location and uncertainties in the actual closure time of the valve and other numerical matters such as mesh or computational element refinement near the valve are not a concern. Not only Novel Model predicted the exact right moment of inception and location of the column separation, but it also predicted the rejoining of the column with less than 2% error compared with the experimental results reported by Sanada et al [4]. Third cause in our provided list is studied before by Ghasvari Jahromi et al [1] and the main difference with the scenarios of the current study is that the cases we consider in this paper are all assumed to be isothermal and hence we do not couple the first law of thermodynamics with our governing system of equations for mass and momentum. The production of the results for the last four cases in this list using the novel model is the subject of this paper and are provided in a sequential form in the next section.

RESULTS

APPLICATION OF THE NOVEL MODEL TO COLUMN

[2] We defined a valve closure as sudden if it occurs at least one order of magnitude faster than the reflection time which is defined to be twice its length divided by the speed of sound in the pipe.

[3] (DVCM, DGCM and GIVCM)

SEPARATION IN A FLOWING PIPELINE

The pipeline considered for this study is assumed to be at adiabatic condition. In adiabatic condition, (no trans-thermal heat-transfer) column separation will not be caused by the temperature changes. Four causes from the above list are to be studied isothermally and only with providing the solution to the governing equations (10) and (11). Table.1 summarizes the description of each scenario we are considering for causing the column separation.

Table 1. Summary of the scenarios considered

Scenario#	Description
1	Effect of temporary change of set point on a pipeline with large elevation changes
2	Effect of transient event (caused by a rupture upstream of segment under study) in a pipeline with large elevation changes
3	Effect of shut-down in a pipeline with large elevation changes followed by a short period of isothermal shut-in
4	Effect of leak event in a pipeline with large elevation changes where a leak could produce column separation near the location of leak.

DESCRIPTION OF THE PIPELINE

The pipeline studied in this paper is a crude oil pipeline with the outside diameter of 30 inches. There are 12 intermediate pump stations in addition to an injection pump station and a delivery terminal. Only one segment of the pipeline which is 53km-long (33 miles) was considered to study the column separation in detail for this paper. This pipeline transports Western Canadian Select (WCS) crude oil. The pipeline elevation profile has a summit which was placed intentionally around the middle of the pipeline. A summary of all the parameters considered in the study is given in Table 2.

Figure 1 shows the elevation profile versus distance for the segment of the pipe considered. The peak visible in the figure is referred to as the summit.

In the next section, we first begin with a brief explanation on the nature of each of these scenarios and provide an initial description of the results of each scenario presented with figures. More discussions are given after all scenarios are described by comparing the differences in the evolution of each column separation scenario and the interfacial mass transfer rates associated with each of them.

Table 2. Characteristics of the system under consideration

Property:	Value:
Main pipeline Temperature	15 ◦c (59 F)
Pipe outer diameter	762 mm (30 in)
Pipe wall thickness	10 mm (0.4 in)
Hydrocarbon liquid density	920.4 kg/m^3 (57.5lb/ft^3)
Hydrocarbon vapor density	2.5 kg/m^3 (0.16 lb/ft^3)
Hydrocarbon liquid viscosity	202.2 cP
Hydrocarbon vapor viscosity	0.0261 cP
Speed of sound in the fluid	1417 m/s (4649 ft/s)
Pipeline length	53.02 km (33 miles)
Vapor Pressure	37.4 kPa (5.4242 psi)
Pipe roughness	45.7 μm (0.0018 in)
Fluid bulk modulus of elasticity	1.67 GPa (2.4e+5 psi)
Pipe Young Modulus of elasticity	167 GPa (2.4e+7 psi)
Ambient Pressure	97 kPa (14 psi)

Scenario#1

At the beginning of this 2-hour-long scenario the pressure drops at the injection site, due to the pump failure (power loss or mechanical malfunction) and causes column separation in the downstream. The proposed model in this paper captures the vapor formation instance, its accumulation at the peak and extension along the pipe. After an hour the problem resolved, and the pressure recovered to its normal operating condition. The model shows how the columns rejoin and the bubbles collapse. When two separated columns rejoin, the released energy caused by the collapsed bubbles causes high local pressure which can be destructive, therefore the operators need a full knowledge of the column inception and evolution make sure column separation is managed properly.

Figure 2 shows the flow rates and pressures used as boundary conditions at both ends of the pipeline for the novel model. Figure 3 shows the hydraulic gradient line versus distance for the segment of the pipe considered at three instances. This clearly shows the state of the line at the beginning and end of the considered scenario as well as the moment at which maximum vapor presented in the system.

Figure 4 compares the predicted pressure at the beginning and end of the scenario along the length of the pipeline. Results

are compared against the predictions of the simulator used for generation of the boundary conditions of the case (i.e. Figure 3). This is done to be sure of the consistency of the hydraulic parameters predicted between the two before relying on the other extra results obtainable only by the new model.

Figure 5 shows the important result of slack line in the form of a contour presentation of the liquid fraction as a function of space and time. Contour plots give a better representation of intensity, location, evolution and fate of the slack. Also, the same contour will be used to compare the fate of this scenario with the other scenarios which slack condition has occurred due to a different transient cause.

Scenario#2

In this scenario, the pressure drops because of a leak event that leads to forming column separation. The total running time of the scenario is 35 minutes. A large size leak (rupture) occurred a few minutes after the start time of scenario. The leak happens in the upstream of the pipeline segment where column separation would take place. The negative pressure wave traverse along the pipeline causing the downstream pressure to drop below the fluid vapor pressure at the highest elevation point.

Figure 6 shows the flow rates and pressures used as boundary conditions at both ends of the pipeline for the novel model under the transient conditions caused by a rupture in the upstream segment of the pipeline segment considered for the study.

Figure 7 shows the spatial-temporal evolution of liquid fraction. Contour plot of the liquid fraction up shows the new intensity and fate of this scenario. As it is clearly shown, the values of liquid fraction in the contour has continued to remain below one until the end of simulation and therefore the cavitating zone is not enclosed like the one seen in the figure 5.

Figure 8 compares the predicted pressure at the beginning and end of the scenario along the length of the pipeline. Results are compared against the predictions of the simulator used for generation of the boundary conditions of the case (i.e. Figure 6). This is done to be sure of the consistency of the hydraulic parameters predicted between the two before relying on the other extra results obtainable by the novel model.

Scenario#3

The third scenario examined the vapor phase embedded in the fluid column during shut-down followed by a short isothermal shut-in period. This is an hour-long scenario with the shut-down process started at the beginning of it. The effects of temperature drop during the shut-in period was subject of our previous work and discussed in detail in [1].

Figure 9 shows the boundary conditions of this transient scenario. These boundary conditions and the state of the line at the beginning and the end of the scenario are shown in Figure 10.

Figure 11 shows the birth of tiny amount of bubbles and subsequent collapse of them. While isothermal conditions considered here have not allowed bigger cavities to be incepted and grow, other cases of shut down followed by transient thermal cooling can cause completely different size of vapor cavities and hence completely different fate of the slack line.

Scenario#4

In this scenario leak happens within the studied segment, a few kilometers upstream of the peak and causes the column separation at the peak. After half an hour duration, a pump was started to study the effect of operator decision to start a pump to bring the column back.

Figure 12 shows boundary conditions of the scenario.

Figure 13 shows the presence of column separation at two different locations for this case. It is important to remember that while initially more than one location may exist with favorable condition for slack line, tendency of deposition of the whole amount of vapor from one location with lower elevation head to the other with higher elevation head is not odd. Especially, when the locations are close together or when there is enough time for one of the locations lower than the other in terms of the elevation height, the lower peak location to be first fully filled with unstable cavity pocket. In the due course there will be no more room locally available at the lower peak location, hence they advect to a higher peak location due to saturation of the lower one by the means of buoyant forces. Such case has been demonstrated by Ghasvari Jahromi et al [1] for cases of slack due to long enough thermal cooling during pipeline shut-in.

Figure 14 shows the pressure profile at the end of this scenario #4. Two locations have reached to the vapor pressure that are located at the highest peaks of the system. (i.e. summit point of the profile and the next highest peak after that).

Figure 15 shows the liquid fraction along the length of the pipeline alongside the volumetric flowrate for the scenario at the end of the simulation of the scenario. The figure shows that the boundary conditions are met only by presence of a sudden drop in flow upstream of the first incepted cavity zone that can only occur due to the leak in the considered model. Figure shows a rupture located at 20 Km (12.4 mile) along the length of the pipeline slightly upstream of the summit.

Comparison of the inception, intensity, evolution and final fate of the captured slack for all four scenarios considered using the novel model.

Figure 16 shows the Inception, evolution and the annihilation of vapor bubbles for scenario #1. About 10 minutes after the scenario began, the column separation has started at the summit and reached the maximum intensity of 0.65 after 50 minutes and then the extra pressure provided to compensate for the lack of pressure has started to rejoin the column in the next 30 minutes and continued as fully liquid again for the remainder of the simulated scenario.

Figure 17 shows that for scenari#2 the rupture upstream of segment under study has incepted cavity at the summit of the pipeline. The cavity has kept growing until the end of the simulated scenario. Even though after the passage of the same amount of time compared to scenario#1, the proportion of the cross-sectional area of the pipeline which has occupied with vapor was less for the second scenario but as it can be clearly seen, the growth has continued until the end of the simulation as the upstream rupture is still causing the loss of fluid and pressure. The vapor cavity zone kept growing to 15% by the time simulation completed.

Figure 18 shows the local inception and very quick annihilation of the incepted bubbles at the highest peak available in the elevation profile of the pipeline due to the shut-down scenario#3. The iso-thermal continuation of the simulation for a short time after the shut-down shows that the column separation can be very negligible compared to fully separated columns observed for the same practice of shut-down and if it continued for extended time with loss of heat to the ambient [1].

Figure 19 shows the evolution of two incepted cavity zones for the last scenario which happened due to leakage within the segment under study. It should be noted that even though both locations are showing the continuous growth of their local cavity zones, but once one reaches fully separated column, it will try to send all its bubbles to a more stable point along the profile if possible. A location with higher altitude in the profile provides higher stability, and buoyant forces help in migrating bubbles between the two locations. This has been observed in the simulation of extended shut-in case as well [1].

Comparison of the interfacial mass transfer rates for all four scenarios considered using the novel model

Direct calculation of the density field over the entire length of the simulation and the pipeline provides the possibility of reporting the interphase mass transfer rate between liquid and vapor directly. It is basically the time rate of change of density of the fluid at any numerical cell multiplied by the volume of that reach.

Figure 20 shows the very transient mechanism of phase change due to set point changes reaching a maximum evaporation rate of 0.75 kg/s (1.65 lb/s) which is followed to reduce to one third of this initial mass transfer rate from liquid to vapor steadily until the second set point change has caused deposition of liquid back to the cavitating zone.

Figure 21 exhibits a much smoother behavior of the phase change due to rupture upstream of the segment under study. Some initial fluctuations are observed after the minimum point observable in this figure. These fluctuations are dampened out within 5 minutes which is in the order of magnitude of the reflection time of the segment. This shows that they were happening perhaps due to secondary reflecting waves of the upstream rupture from boundary nodes. Here, also the final rate of phase change reaches to about one third of the initial value of phase change rate.

Figure 22 verifies the instantaneous rejoining mechanism acting in the shutdown scenario. The value of the positive pulse of the phase change as seen in the figure compared to the negative value of the pulse prior to that shows the initial tendency of the system after shutting down to go back to fully liquid phase again.

Figure 23 shows the different rates of evaporation at each of the two peaks where column separation has occurred. It is clearly showing one initial condensation at the higher peak. The lower peak that was initially growing faster has started to vaporize at a lower rate after a while and an intersection point can be seen further into the simulation between the black and red lines. This is a battle which as we described its fate will be determined finally by buoyancy should it continues towards fully filled cross sectional areas.

Figure 24 shows the flowrates versus time at three different location of the pipeline for scenario#4. The two locations at which column separation is taking place, plus at the spotted leak location. It shows how the startup of a pump by an operator to rejoin the column has not been effective (Operator being unaware of the incepted leak assumes the column separation from experience and tries to rejoin the column that operator thinks has occurred due to loss of power by starting a new pump or adding more pumping power to the upstream end of the pipeline).

Figure 25 shows the column separation in the horizontal pipeline using the novel model for the case of mid-stream cavitation in a horizontal pipe with sudden pressure drop in the upstream end of the pipe. The birth and death marks on this figure are coming from the experimental study [4].

As we can see there is a very good agreement between the measured time of birth and death of the bubbles by experiments and the predicted ones at the same location using the proposed novel model in this paper. The transient cause of column separation for the scenario#1 considered in this paper is very similar to the results of the novel model validated against this experiment.

We consider such order of accuracy in the spatial prediction and time evolution of the column separation phenomenon to be enough for studying the applied industrial scale scenarios and hence we proceed to the conclusions from the current study.

CONCLUSIONS

A novel mathematical model for the phenomenon known as column separation or slack line was provided. This model was used in an industrial scale virtual pipeline after being validated [1] against benchmark experimental results.

Cases of column separation due to transients of different nature were studied. Contours of liquid fraction which determines the vapor and liquid fractions at the cross-sectional area of the pipeline were generated. The contour plots of this type can show the cavitating zone over the domain of space and time.

The intensity of column separation in each scenario studied is provided using the time plots of the liquid fraction at the location of phase change.

The novel model was successful in addressing all causes of column separation. The direct calculation of density allowed for the precise prediction of the rates by which phase change happens (whether evaporation to vapor phase or condensation back to the liquid phase)

Generally, the presence of column separation can result in large uncertainty in hydraulic calculations. Because most systems rely on the accuracy of the RTTM for leak detection purposes, they may not be able to detect leaks reliably under slack conditions. Therefore, two out of four scenarios in this paper were designated to the cases where column separation can occur due to leaks/ruptures.
One of the leaks causing the slack line has occurred within the segment under the study(scenario#2) and the other one happened in the upstream segment of the pipeline segment under study(scenario#4).

To the best of the authors' knowledge, the ability of a model in determination of the column separation due to leak/rupture is being presented for the first time.

The distinguishing ability of the novel model in detection of the leak plus its ability to predict the amount of phase change and location of vaporous cavities due to the leak events is also quite unique and has been not reported in the literature. We conclude that the proposed model presented int his paper is reliable for applied hydraulic purposes such as complicated case of slack due to leak (as demonstrated by scenario#4).

REFERENCES

1. Ghasvari Jahromi H, Roxas M, Mokamati S. "Column Separation in a Shut-In Liquid Hydrocarbon Transmission Pipeline", *Proceedings of ASME* International Pipeline Conference, Volume

3: Operations, Monitoring, and Maintenance; Materials and JoiningV003T04A027. doi:10.1115/IPC2018-78743.

2. *A. Bergan, A.R Simpson, 1999, "Cavitation inception in pipeline column separation", Proceedings of the 28th IAHR Congress, Graz, Austria.*

3. *A. Bergant, A.R. Simpson, A.S. Tijsseling, 2006, "Water hammer with column separation, A historical review", Journal of Fluids and Structures, 22, pp 135-171*

4. Sanada, K.; Kitagawa, A.; Takenaka, T. A study on analytical methods by classification of column separations in a water pipeline. Bull. JSME 1990, 56, 585–593.

AUTHOR BIOGRAPHY

Hamed Ghasvari Jahromi Chief R&D Scientist (Column Separation, Leak Detection and Simulations) has years of experience in developing and applying Mathematical Modeling and fluid dynamics theories to Industrial Problems. He has extensive experience in developing leak detection technologies especially column separation prediction models, RTTM, and pattern recognition approaches to leak detection. He also has extensive experience with CFD for modeling flow, Transient flows, Multiphase Flows and Cavitation Analysis.

Fatemeh Ekram is a Process Data Analytics and Control Scientist. Her expertise is in simulating transport phenomena and designing algorithms to control their behavior. She developed predictive control strategies with application in chemical and biomedical engineering. Fatemeh got her B.Sc. and M.Sc. degrees from Sharif University of Technology and completed her Ph.D. at the University of British Columbia in Chemical & Biological Engineering.

Michael Roxas Simulation and Modelling Analyst, has broad experience in pipeline leak detection, simulation and modeling. Obtained a BSc. degree in Chemical Engineering from University of Alberta. Michael's expertise include experience in hydraulics modeling, pipeline simulations, pipeline leak detection testing, and software development.

Satya Mokamati Principal Engineer (leak Detection and Pipeline Simulations) has broad pipeline leak detection, simulation and modeling experience. Obtained PhD in Mechanical Engineering from UBC, Vancouver; MS in Mechanical Engineering from UNB, Fredericton; Undergrad from India. Satya's expertise include experience in hydraulics modeling/ numerical analysis, Pipeline Simulations, Pipeline Leak Detection Testing, leak detection technology development.

FIGURES

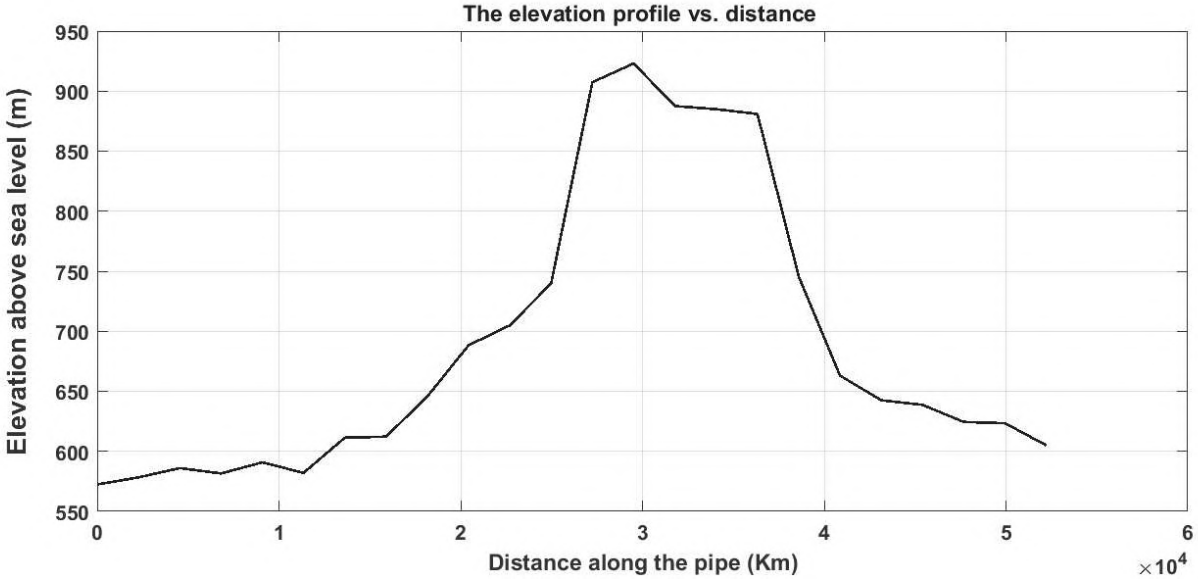

Figure 1 –The elevation profile versus distance for the segment of the pipe considered.

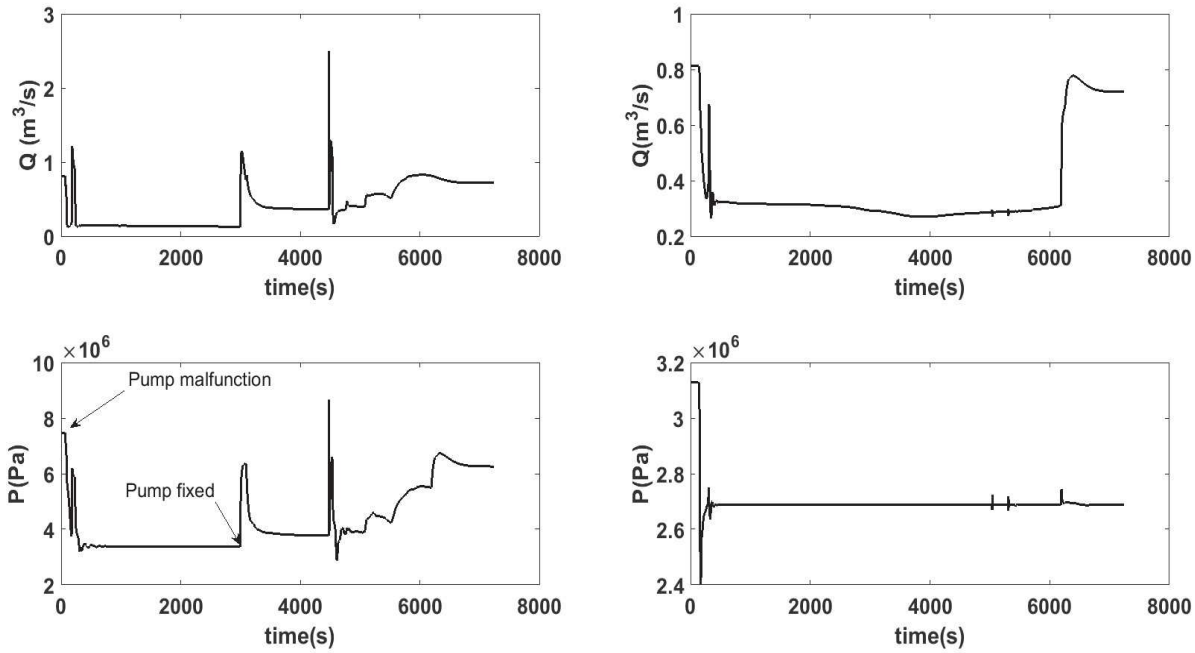

Figure 2 –Flow and pressure boundary conditions for scenario #1

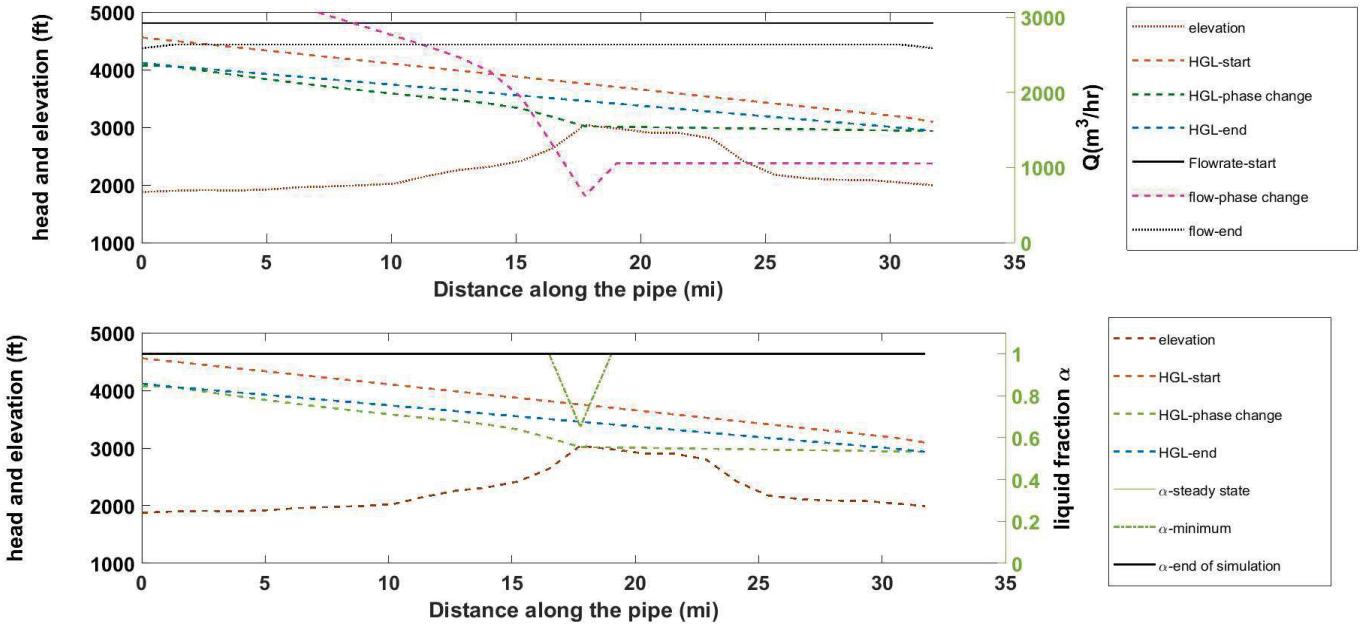

Figure 3. The hydraulic state of the line at three instances (the beginning and end of the simulation and the moment when vapor fraction is maximum inside the pipe.) The figure at the top shows head and elevation on the left axis and the flow rate on the right axis. The figure at the bottom shows head and elevation on the left axis and the liquid fraction on the right axis.

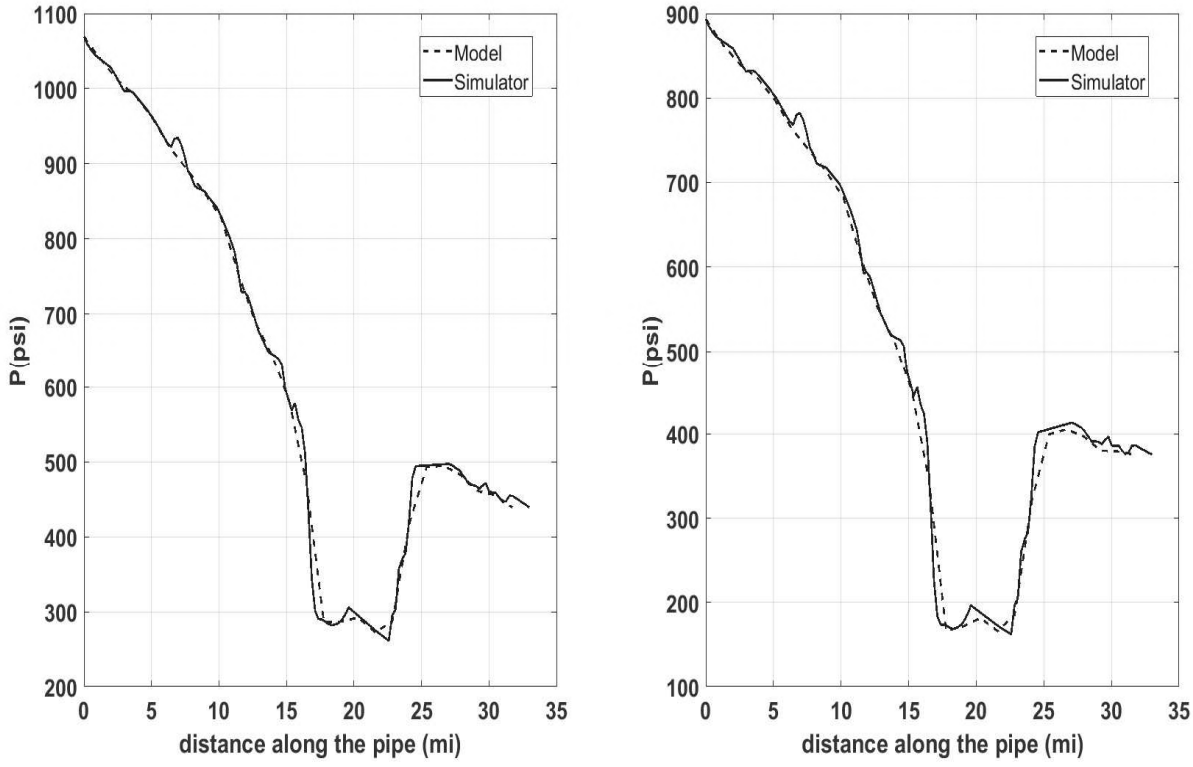

Figure 4. Comparison of the distance plots of pressure at the beginning and end of scenario #1 between the new model and simulator

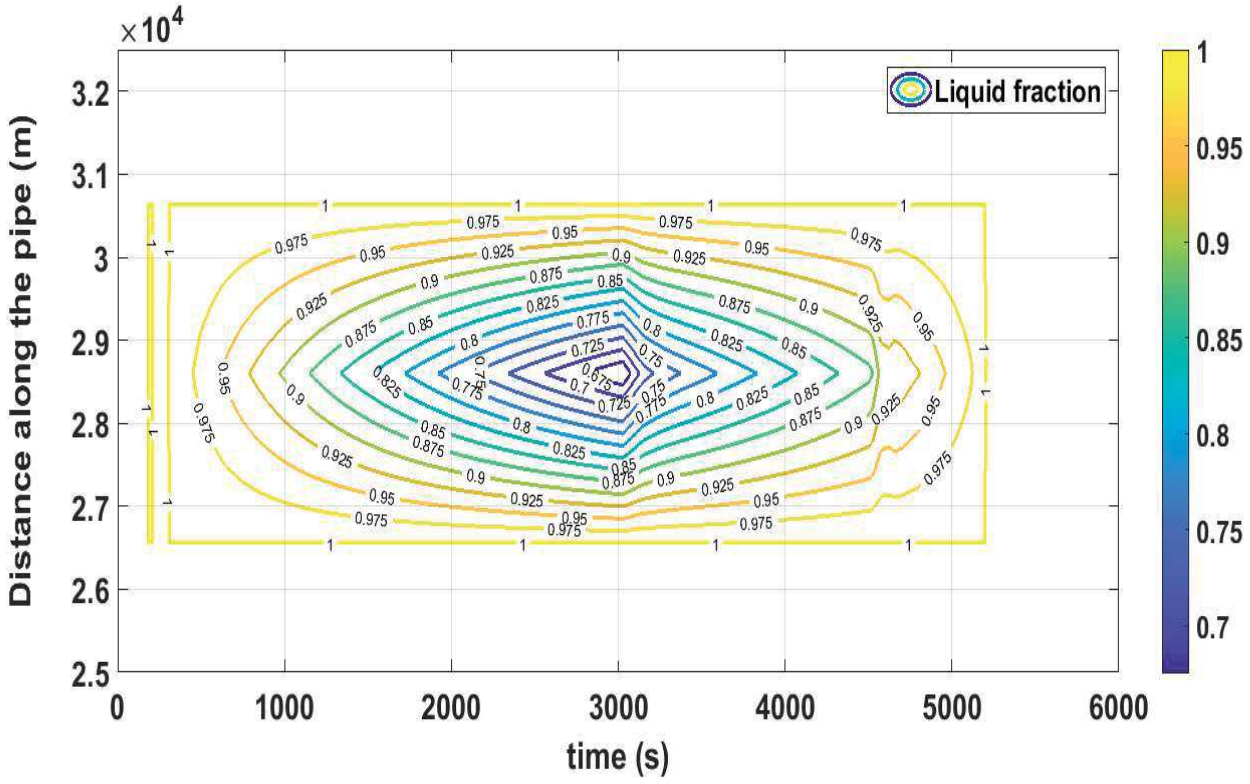

Figure 5. The spatial-temporal evolution contour of column separation for scenario #1 (The values on the graph represent the liquid fraction, the space is on y-axis and the time is on x-axis.)

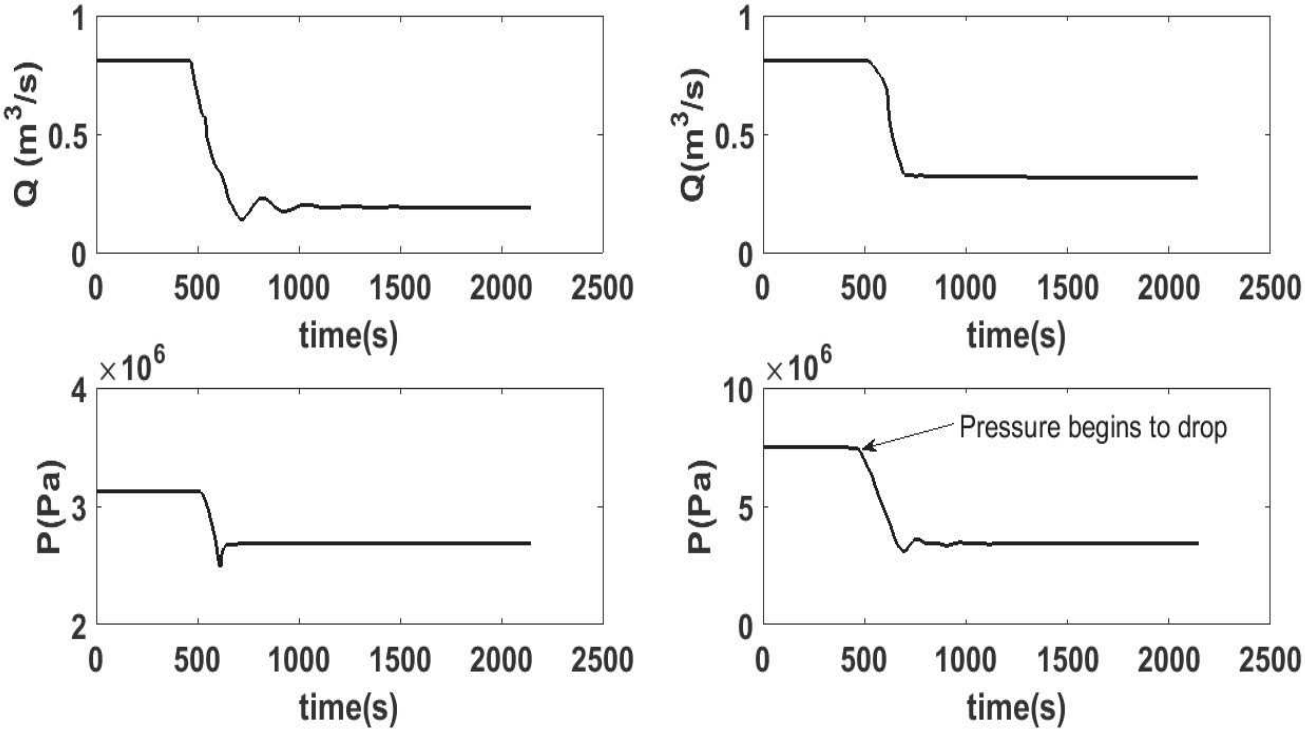

Figure 6 – Flow and pressure boundary conditions for scenario #2

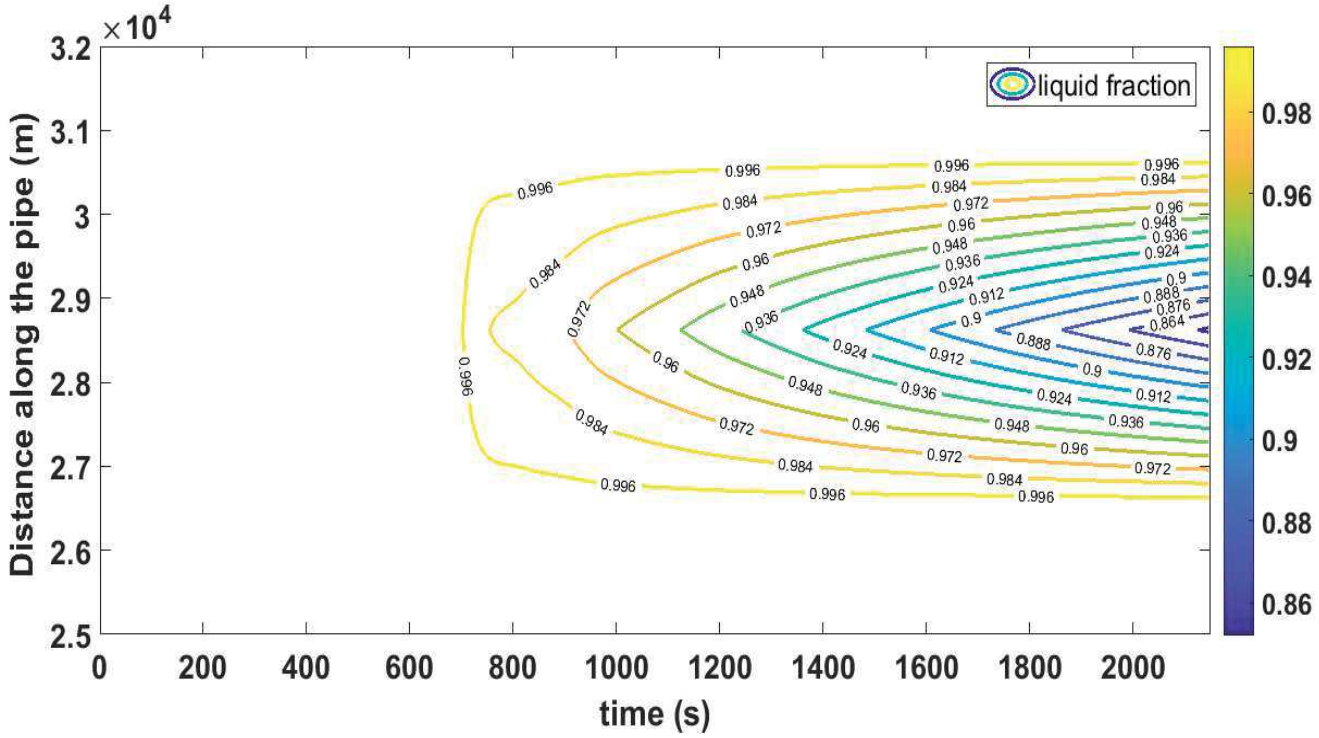

Figure 7. The spatial-temporal evolution contour of column separation for scenario #2. (The values on the graph represent the liquid fraction, the space is on y-axis and the time is on x-axis.)

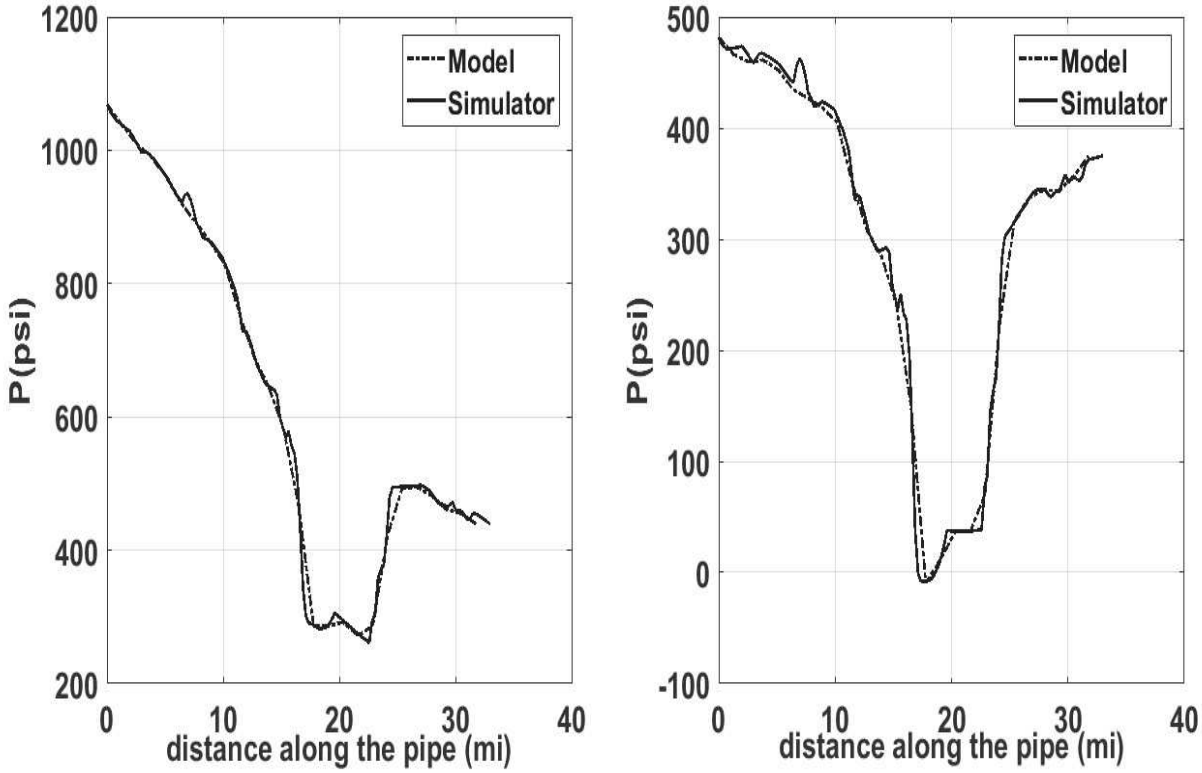

Figure 8. Comparison of the distance plots of pressure at the beginning and end of scenario #2 between the new model and simulator

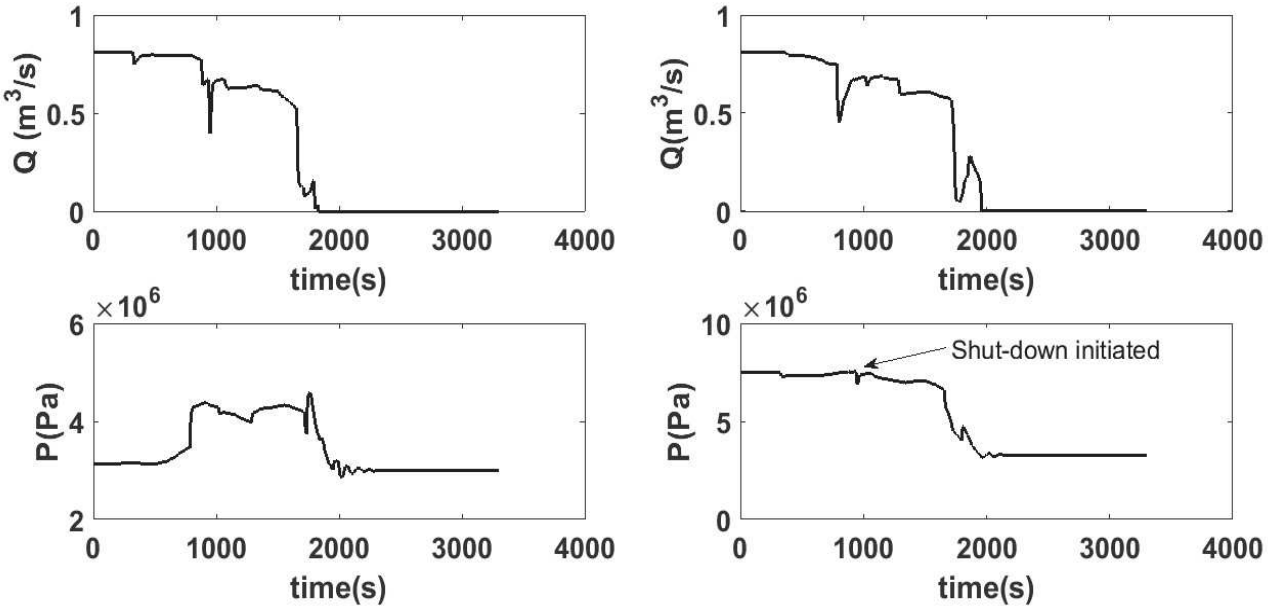

Figure 9 – Flow and pressure boundary conditions for scenario #3

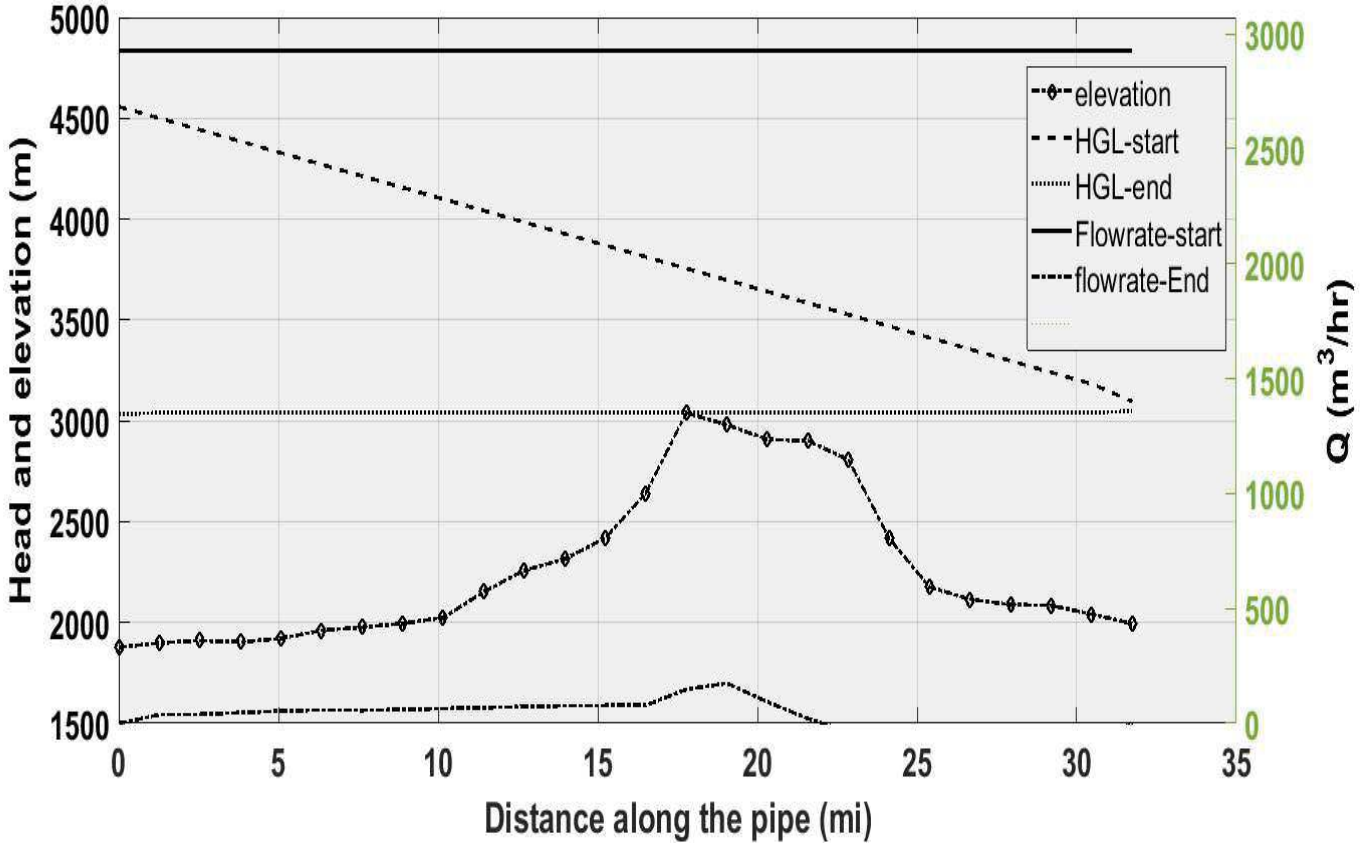

Figure 10- . The hydraulic state of the line at the beginning and end of the simulation along the pipe. The head and elevation are on the left axis and the flow rate is on the right axis.

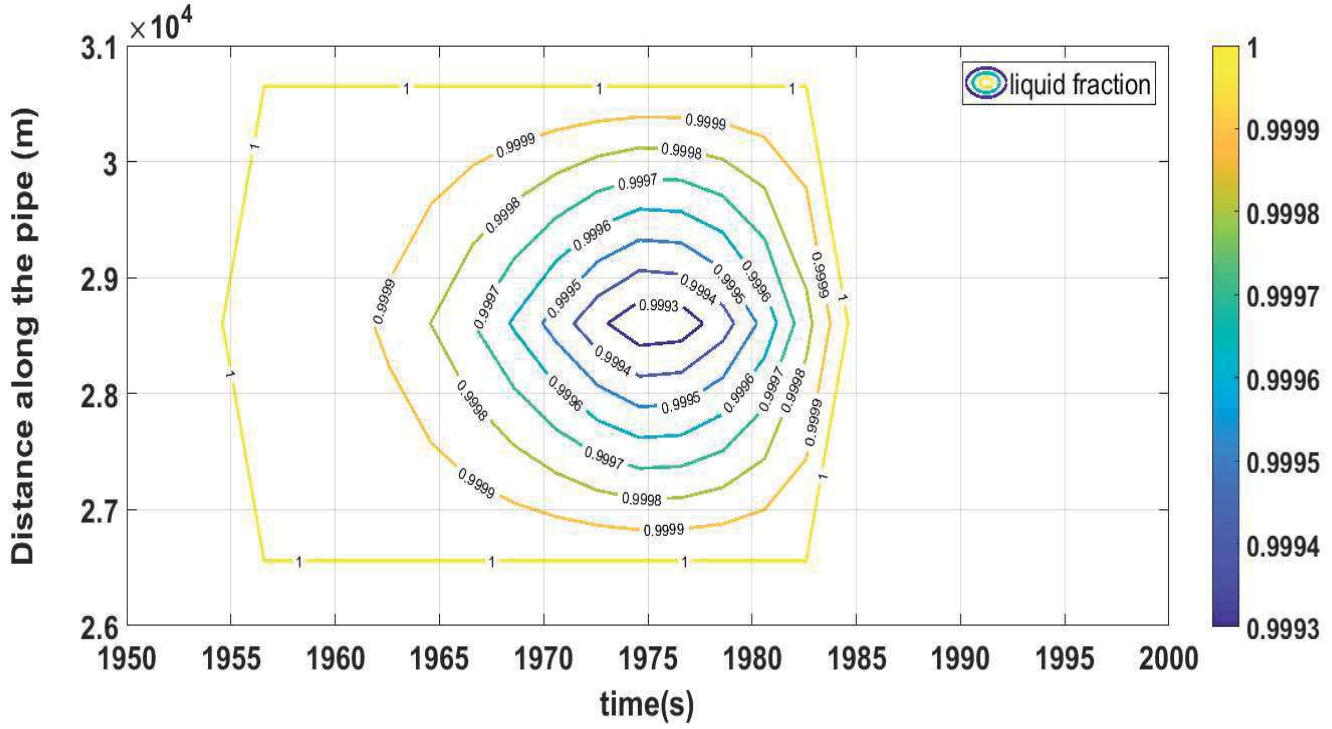

Figure 11. The spatial-temporal evolution contour of column separation for scenario #3. (The values on the graph represent the liquid fraction, the space is on y-axis and the time is on x-axis.)

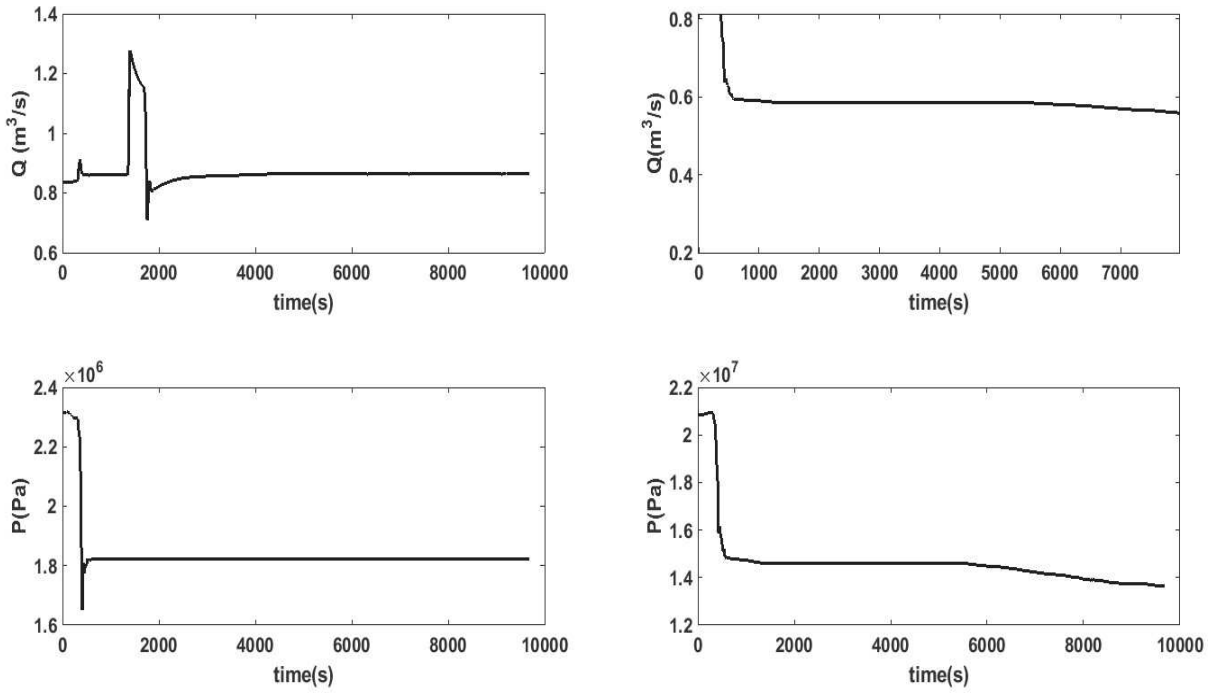

Figure 12 – Flow and pressure boundary conditions for scenario #4

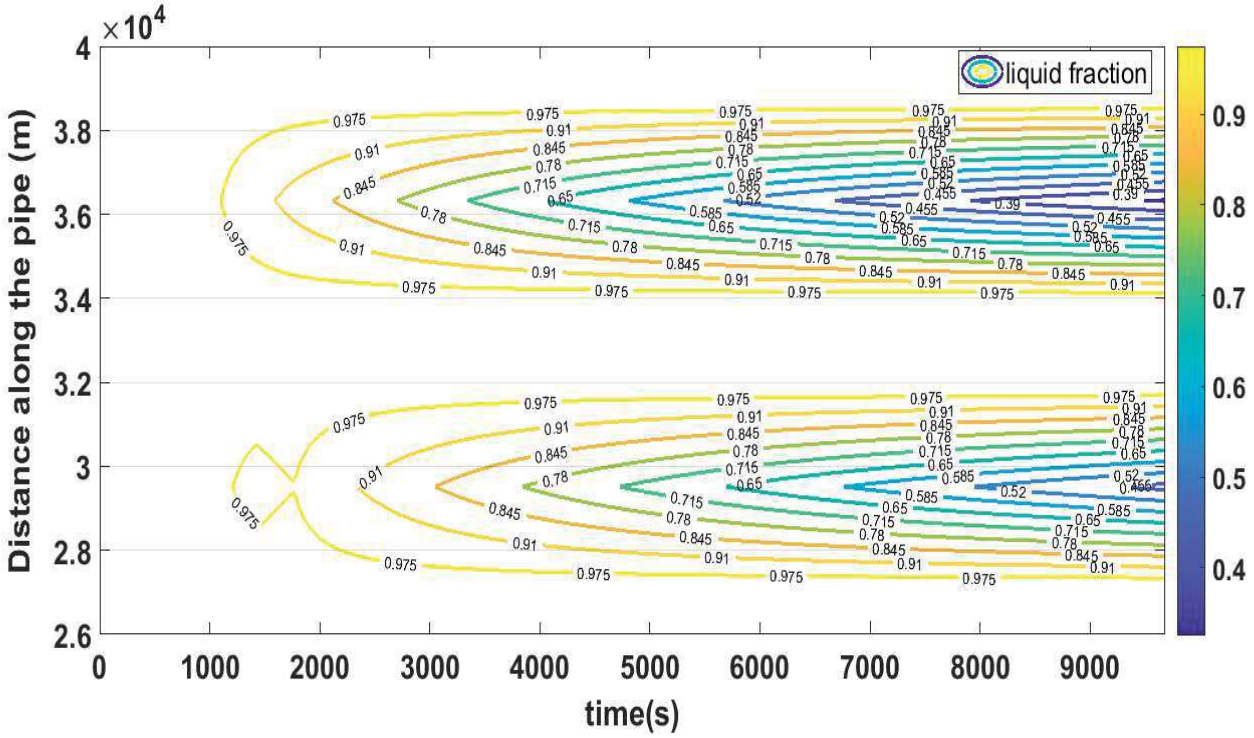

Figure 13. The spatial-temporal evolution contour of column separation at both peak locations for scenario #4 (The values on the graph represent the liquid fraction, the space is on y-axis and the time is on x-axis.)

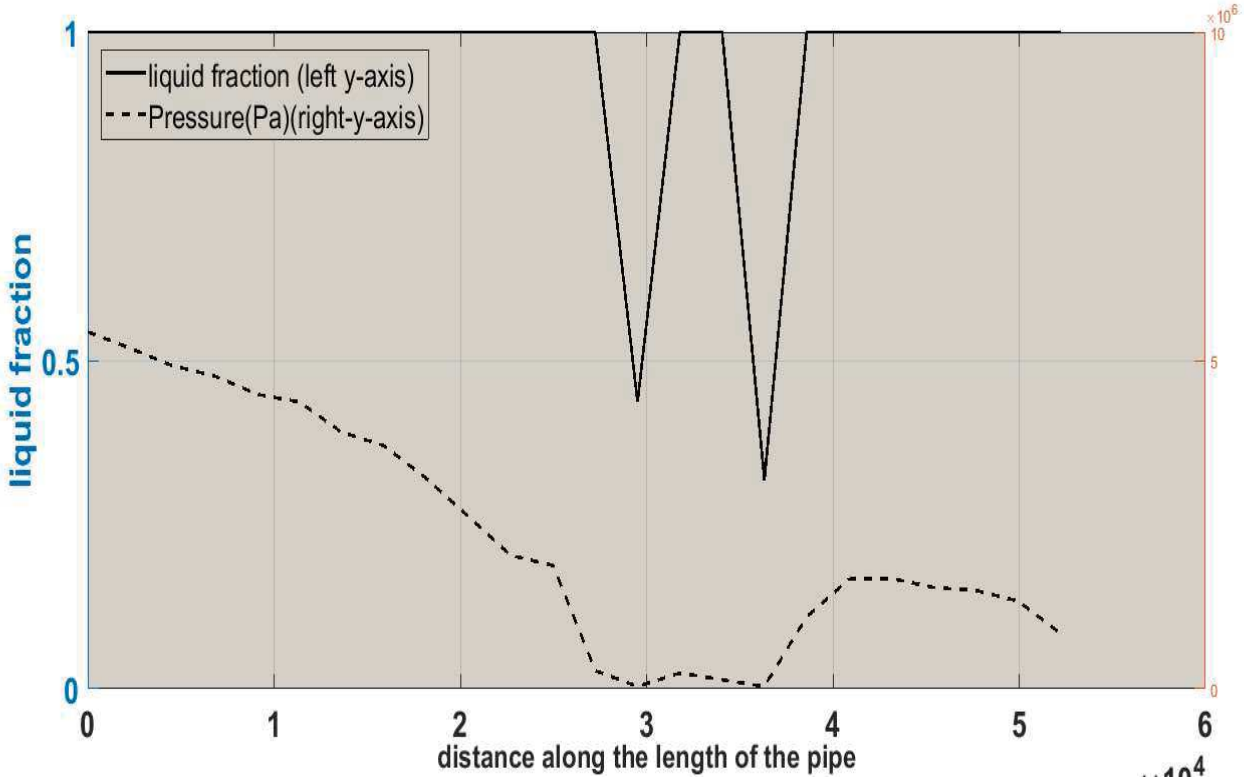

Figure 14. The liquid fraction (dot-dashed black line) and pressure profile (dashed blue line) along the pipe at the end of scenario #4

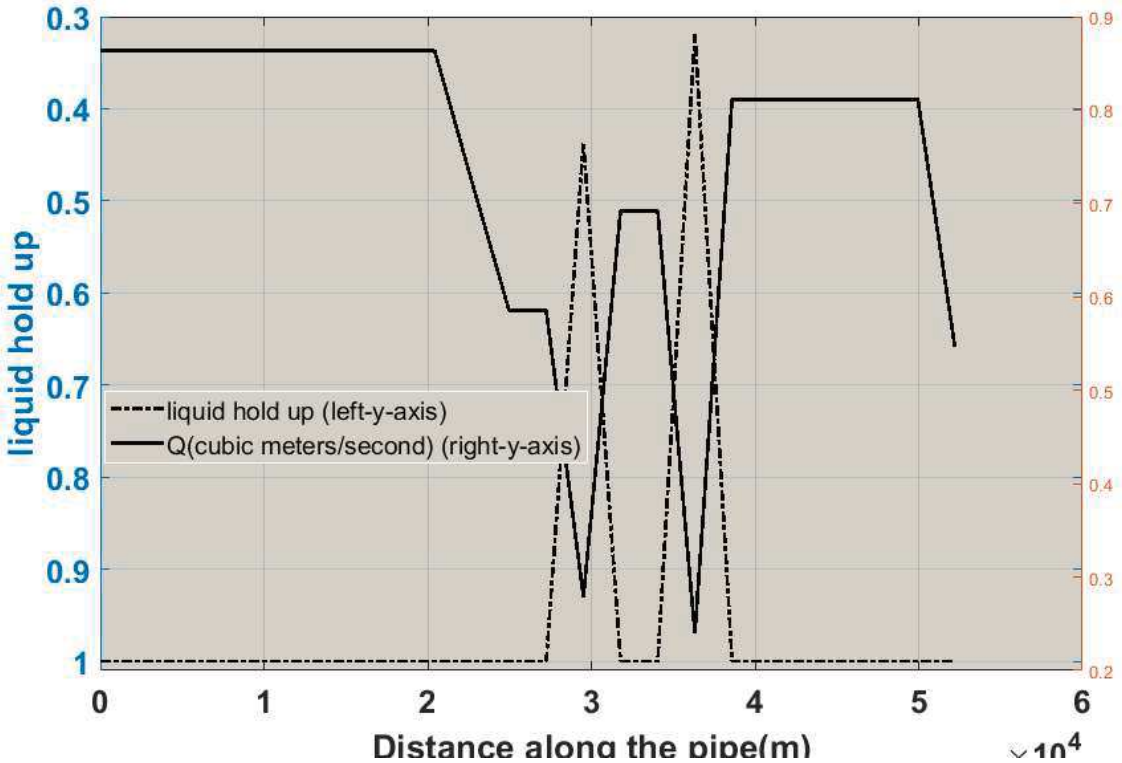

Figure 15. Liquid hold up (dot-dashed red line) on the left axis and flowrate (solid black line) on the right axis along the pipe at the end of scenario #4

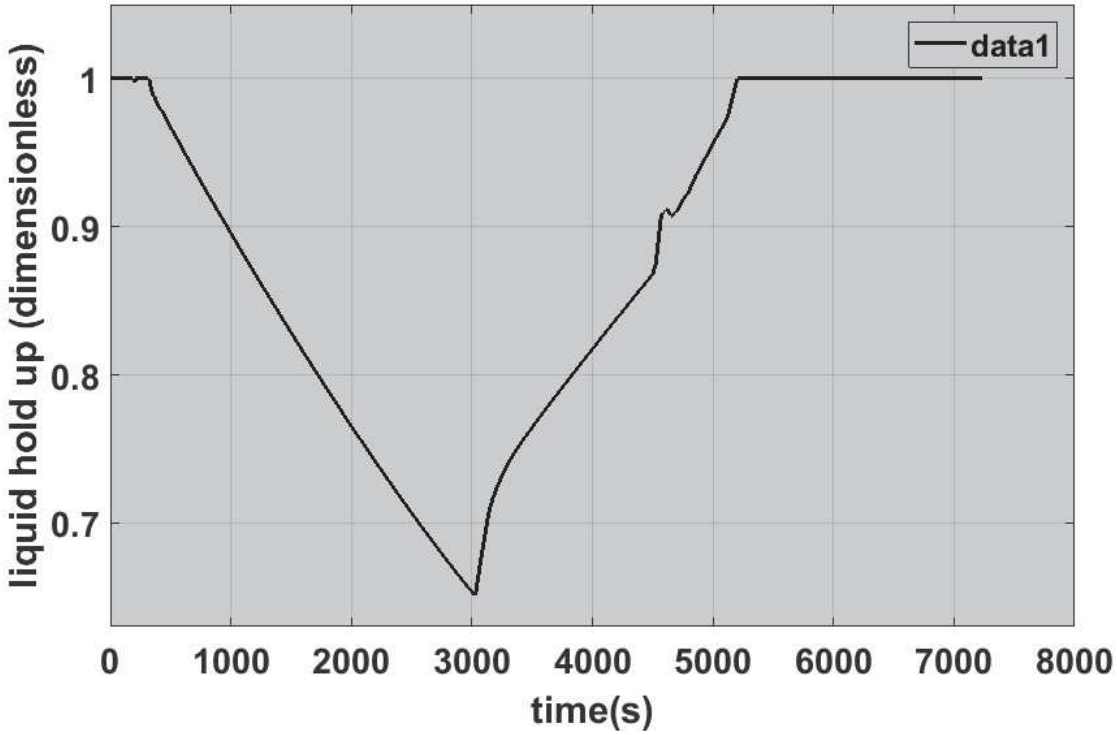

Figure 16. Inception, evolution and the annihilation of column separation for scenario #1 at 28.6 Km of the pipe length

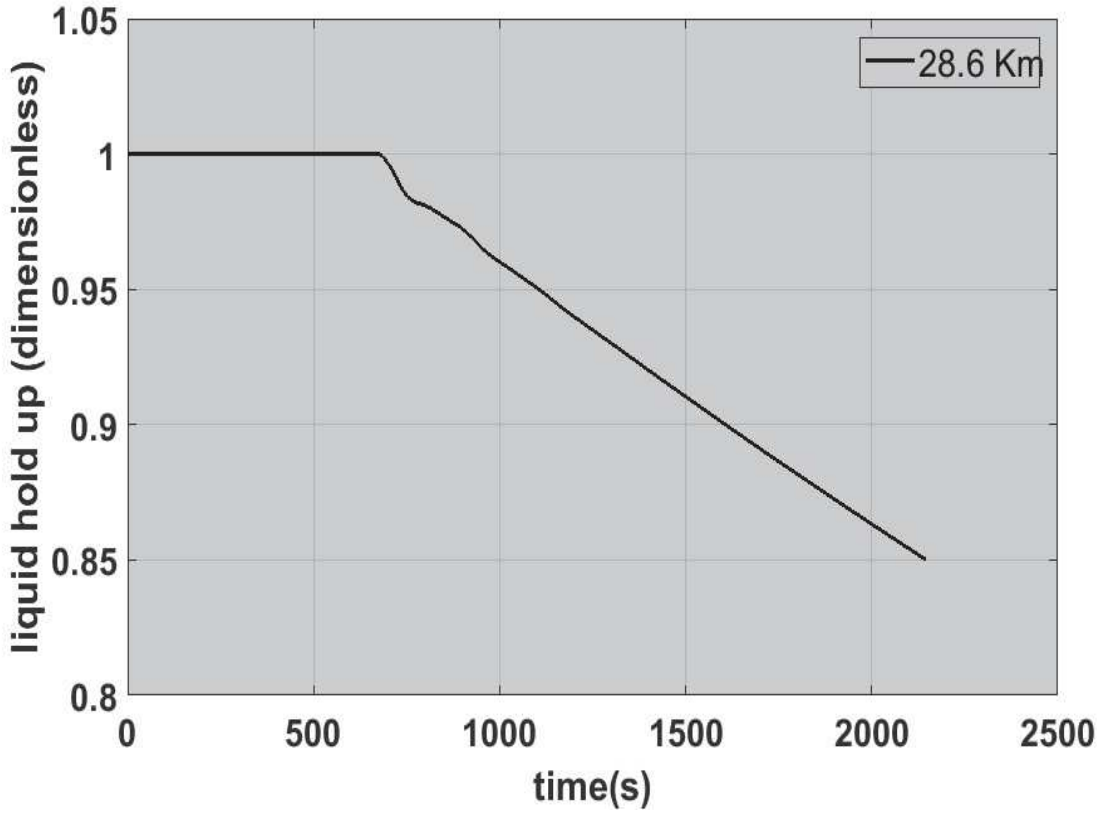

Figure 17. Inception, evolution and the annihilation of column separation for scenario #2 at 28.6 Km of the pipe length

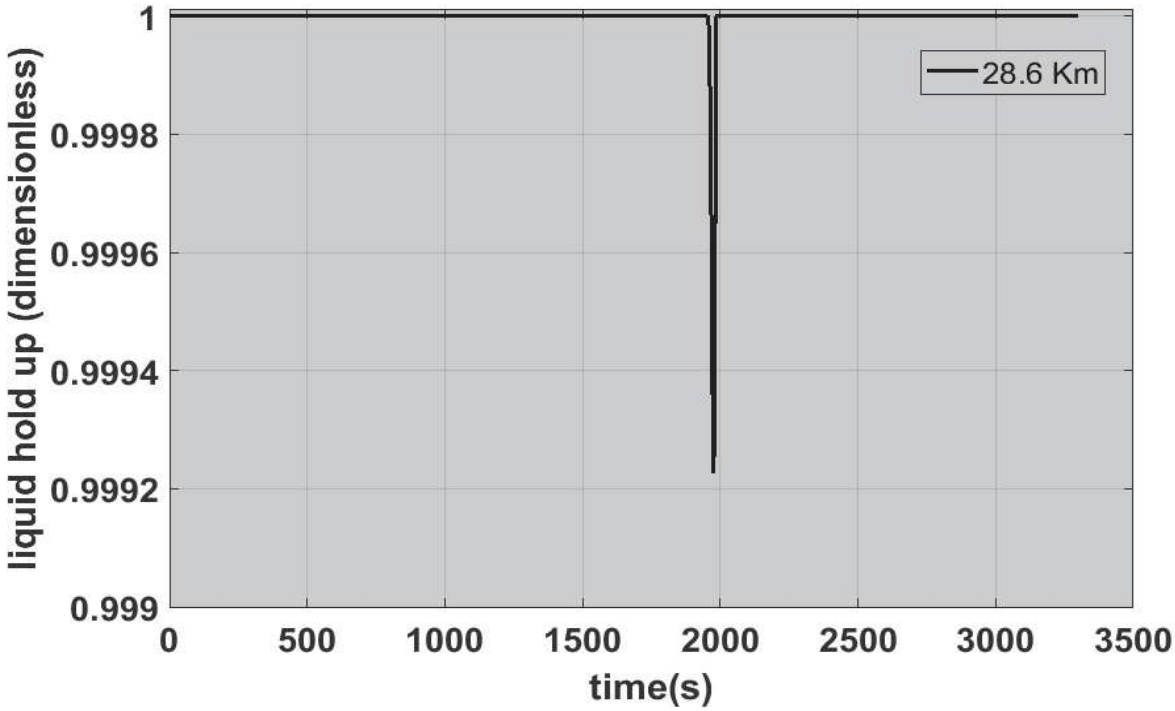

Figure 18. Inception, evolution and the annihilation of column separation for scenario #3 at 28.6 Km of the pipe length

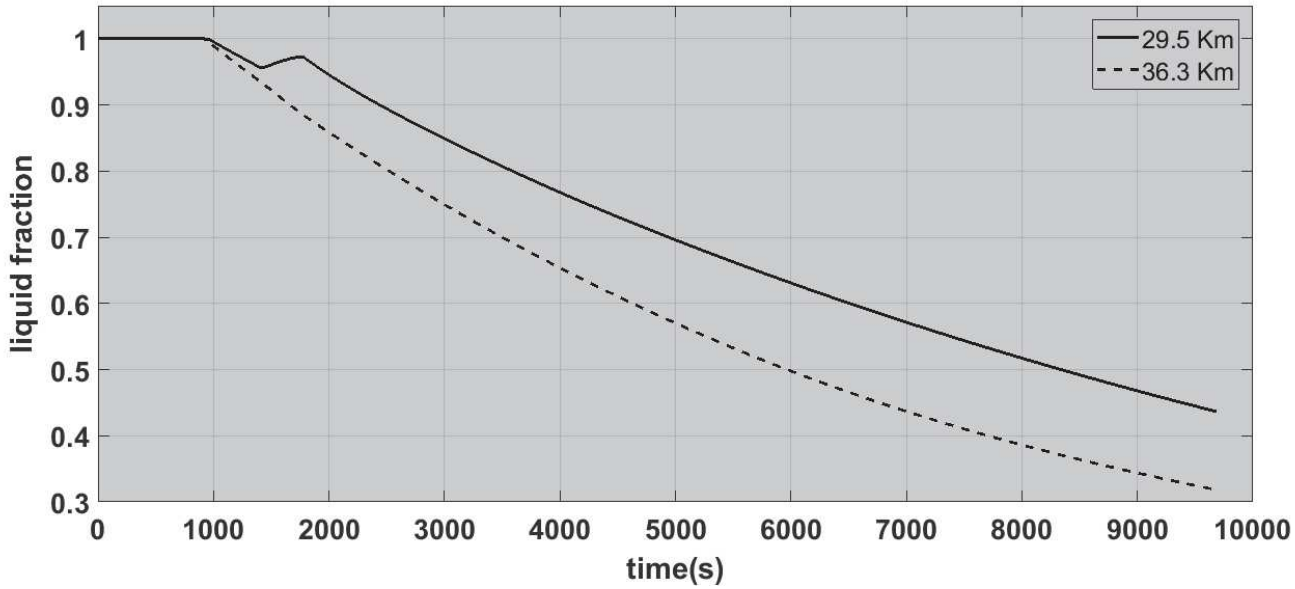

Figure 19. Inception, evolution and the fate of column separation for scenario #4 (dashed black line at 29.5 Km of the pipe length, and the dashed red line at 36.3 Km of the pipe length)

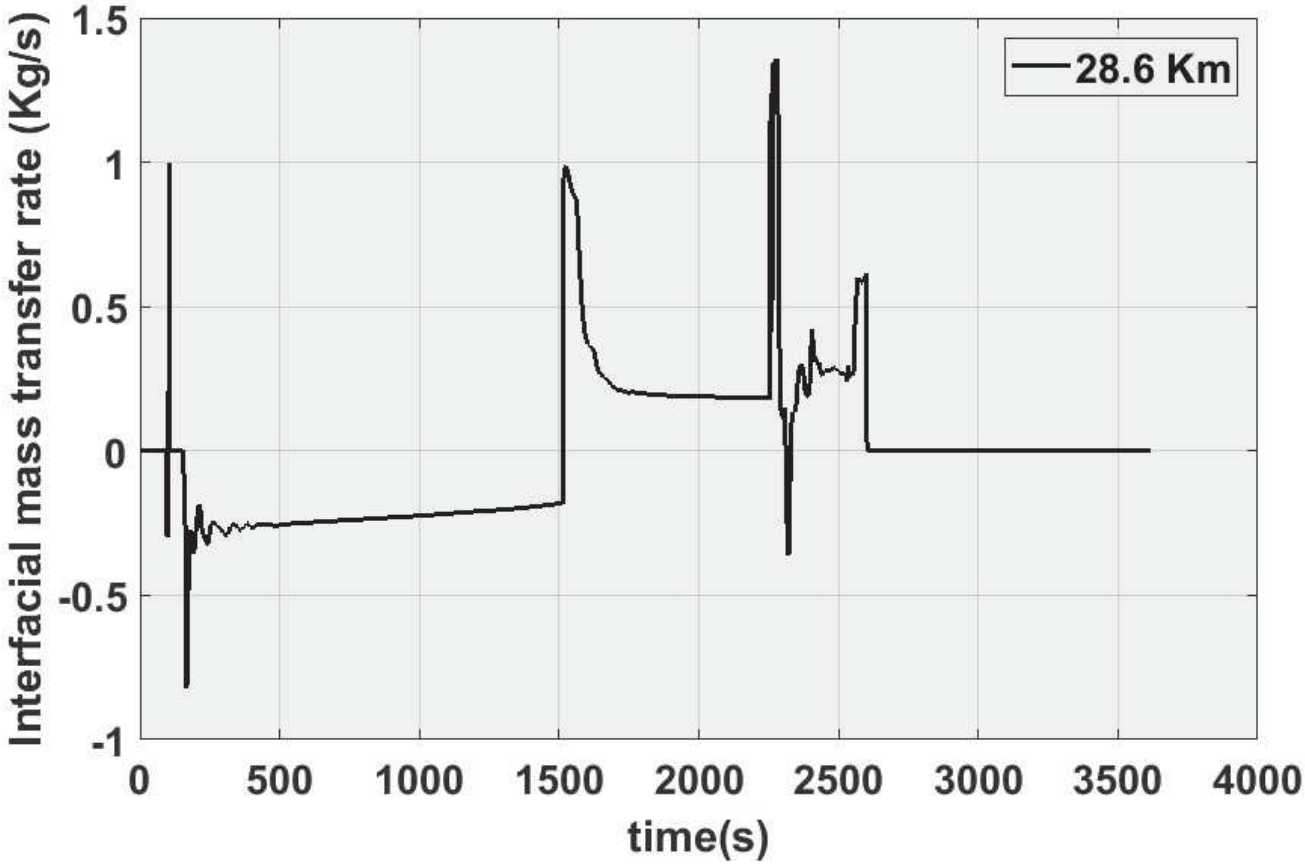

- **Figure 20. The interfacial mass transfer at 28.6 Km for scenario #1**

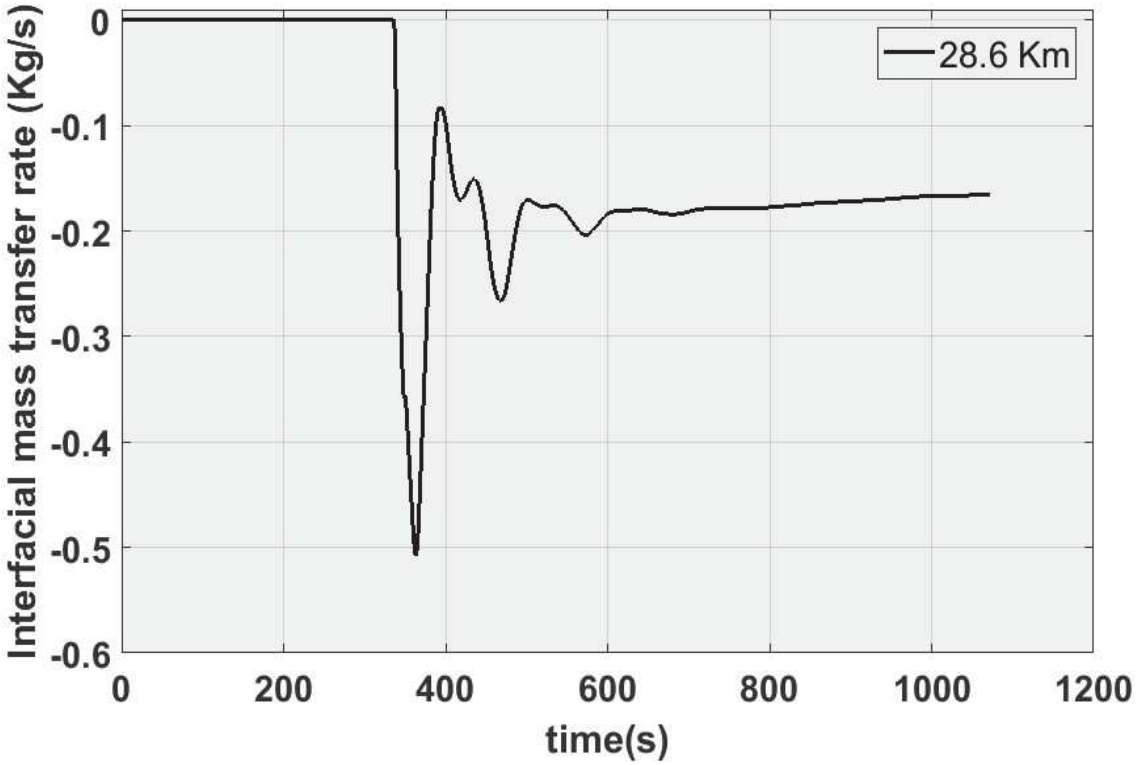

Figure 21. The interfacial mass transfer at 28.6 Km for scenario #2

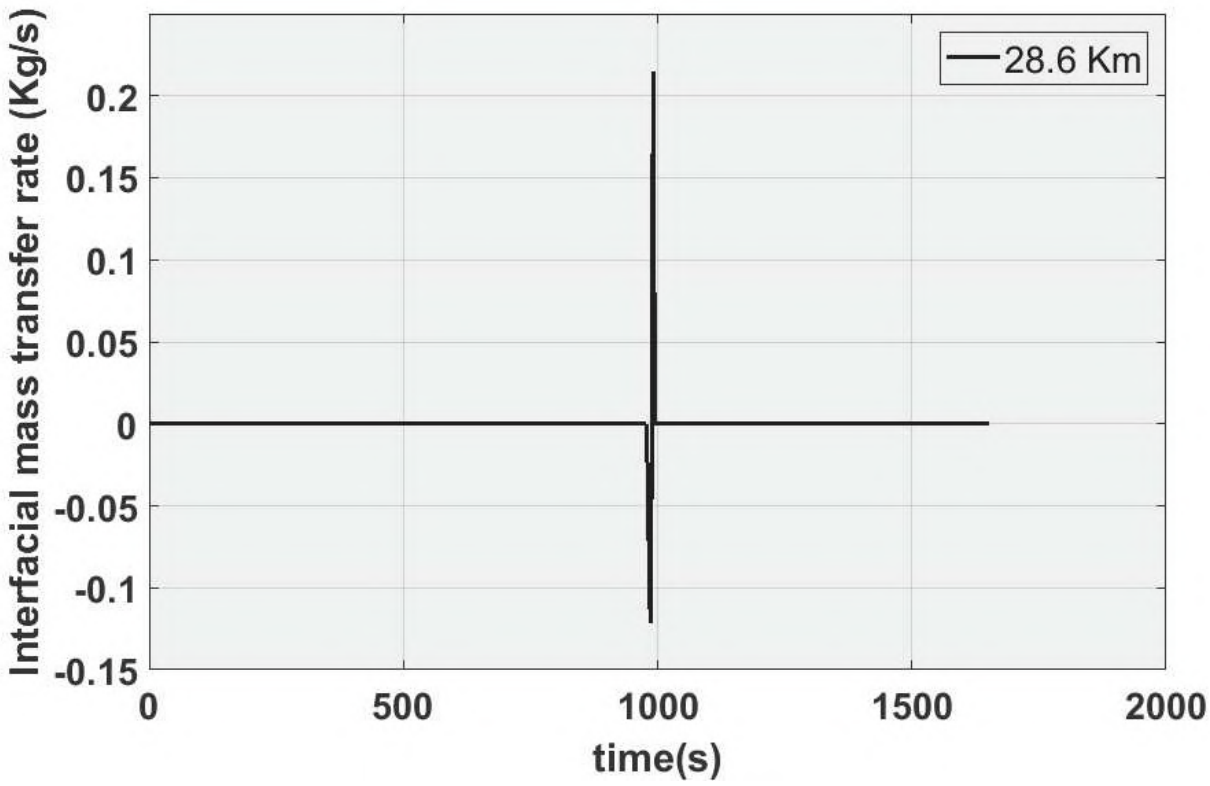

Figure 22. The interfacial mass transfer at 28.6 Km for scenario #3

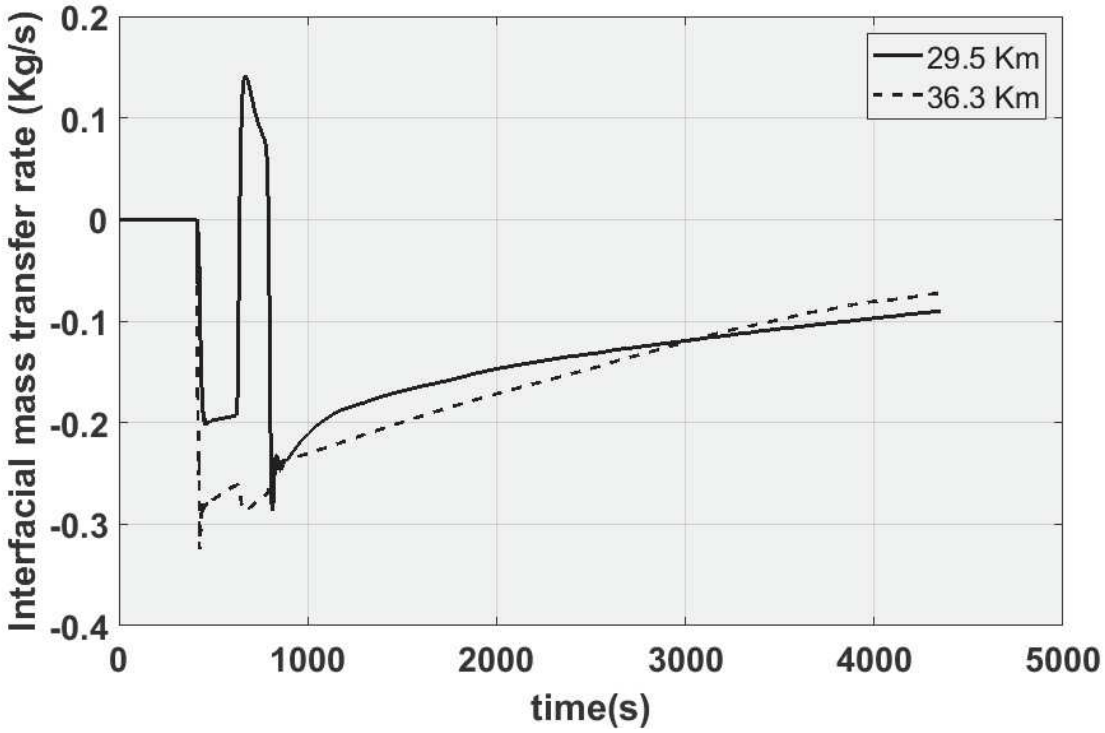

Figure 23 Comparison of the interfacial mass transfer at two locations for scenario #4 (dash-dotted black line at 29.5 Km of the pipe length, and the dash-dotted red line at 36.3 Km of the pipe length)

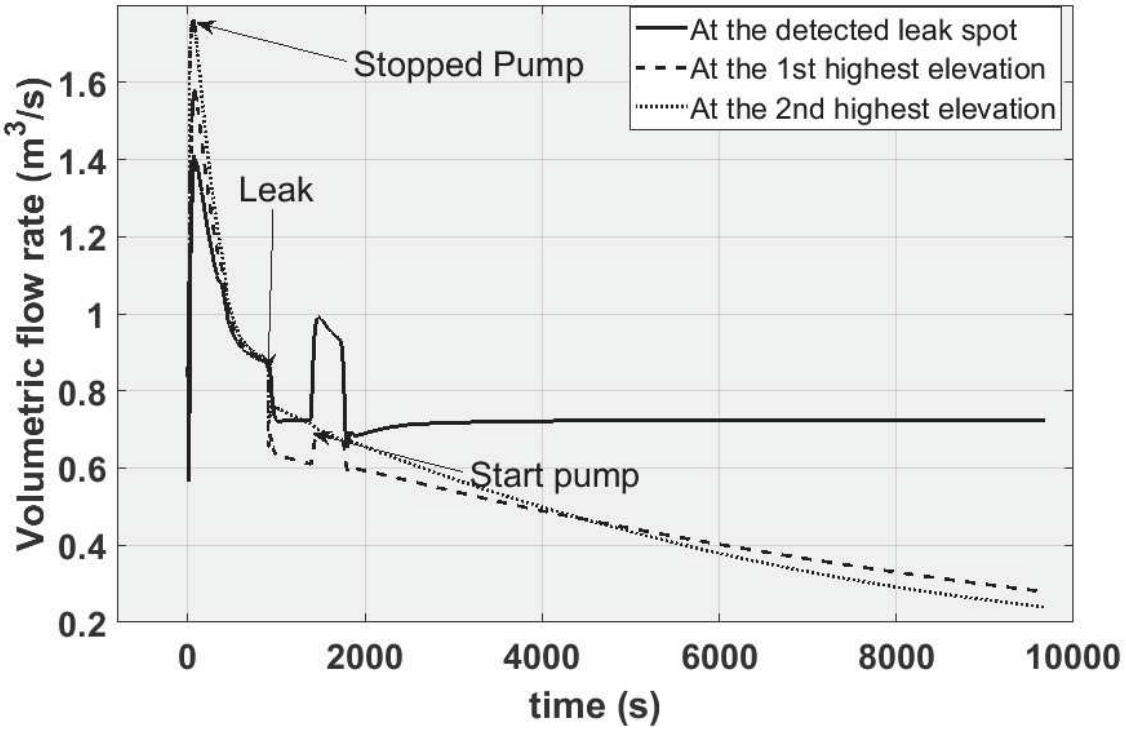

Figure 24. The comparison of the flow rates during the simulation time at the leak location (solid black line) and two peaks (dash-dotted red line for the highest peak and the dashed blue line for the 2nd highest peak)

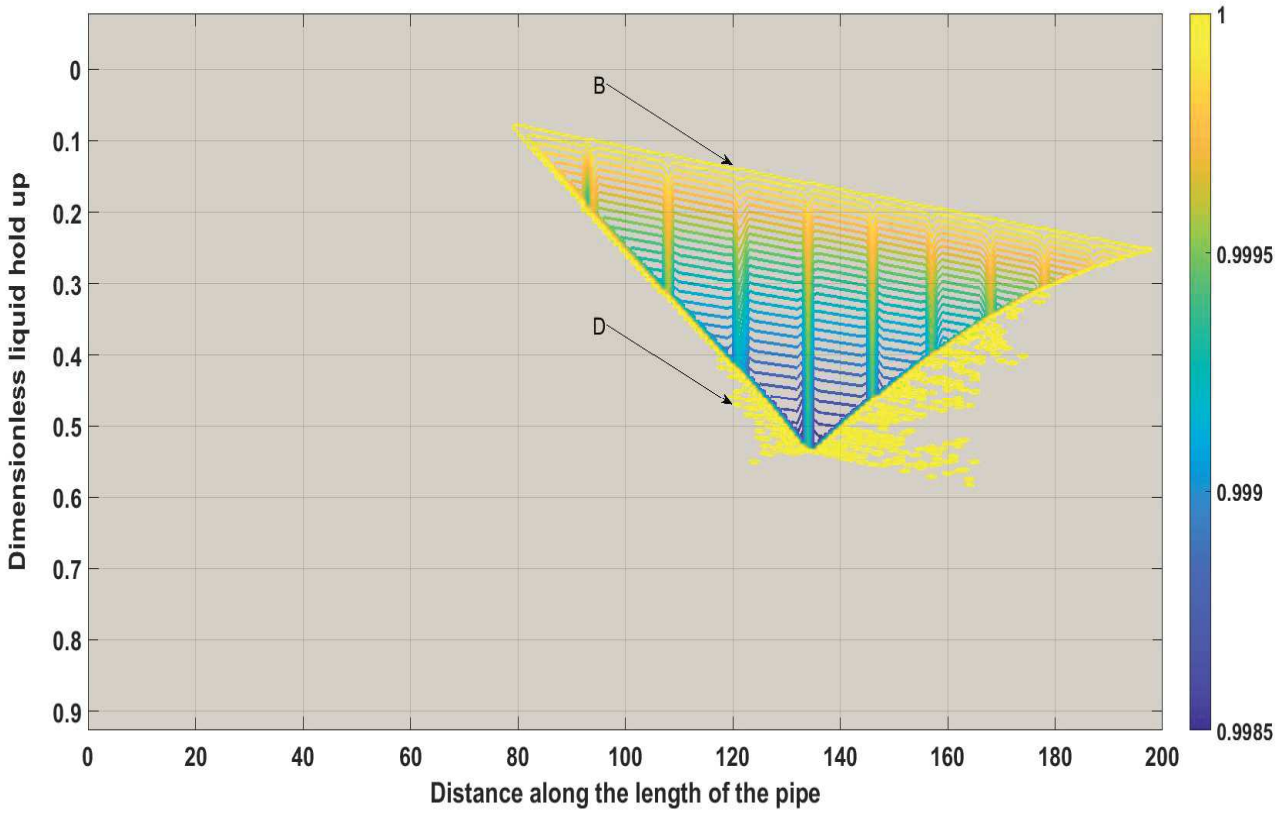

Figure 25. Validation of the proposed model with experimental data